mathematics

Article

Identification of Quadratic Volterra Polynomials in the "Input–Output" Models of Nonlinear Systems

Yury Voscoboynikov [1,2], Svetlana Solodusha [3,*], Evgeniia Markova [3], Ekaterina Antipina [3,4] and Vasilisa Boeva [1]

1 Department of Applied Mathematics, Novosibirsk State University of Architecture and Civil Engineering, 630008 Novosibirsk, Russia; voscob@mail.ru (Y.V.); v.boyeva@sibstrin.ru (V.B.)
2 Department of Automation, Novosibirsk State Technical University, 630087 Novosibirsk, Russia
3 Department of Applied Mathematics, Melentiev Energy Systems Institute, Siberian Branch of Russian Academy of Sciences, 664033 Irkutsk, Russia; markova@isem.irk.ru (E.M.); kate19961231@gmail.com (E.A.)
4 Department of Mathematical Analysis and Differential Equations, Irkutsk State University, 664003 Irkutsk, Russia
* Correspondence: solodusha@isem.irk.ru

Abstract: In this paper, we propose a new algorithm for constructing an integral model of a nonlinear dynamic system of the "input–output" type in the form of a quadratic segment of the Volterra integro-power series (polynomial). We consider nonparametric identification of models using physically realizable piecewise linear test signals in the time domain. The advantage of the presented approach is to obtain explicit formulas for calculating the transient responses (Volterra kernels), which determine the unique solution of the Volterra integral equations of the first kind with two variable integration limits. The numerical method proposed in the paper for solving the corresponding equations includes the use of smoothing splines. An important result is that the constructed identification algorithm has a low methodological error.

Keywords: nonparametric identification; dynamic system; integral model; Volterra equations; smoothing cubic splines; selection of the smoothing option

MSC: 45D05

check for updates

Citation: Voscoboynikov, Y.; Solodusha, S.; Markova, E.; Antipina, E.; Boeva, V. Identification of Quadratic Volterra Polynomials in the "Input–Output" Models of Nonlinear Systems. *Mathematics* **2022**, *10*, 1836. https://doi.org/10.3390/math10111836

Academic Editors: Natalia Bakhtadze, Igor Yadykin, Andrei Torgashov and Nikolay Korgin

Received: 12 April 2022
Accepted: 24 May 2022
Published: 26 May 2022

1. Introduction

The development of the theory of dynamical systems, taking into account the specifics of applied problems, aims to create new mathematical methods. This paper is devoted to the develop mathematical tools for studying inverse problems in the theory of dynamical systems. The work aims to develop a methodology and algorithms for identifying Volterra polynomials (finite segments of Volterra series) [1].

$$y(t) = \sum_{n=1}^{N} \int_0^t \ldots \int_0^t K_n(t, s_1, \ldots, s_n) \prod_k^n x(s_k) ds_k, t \in [0, T]. \tag{1}$$

The Volterra integro-power series is well known in the theory of mathematical modeling of nonlinear dynamic systems of the "input–output" type. However, modern and classical studies in this area do not provide a universal mathematical apparatus for studying problems with restrictions on the dynamic characteristics of systems.

Reference [2] contains an extensive list of references on methods for identifying nonlinear objects using Volterra integral equations. References [3–7] are devoted to methods for constructing dynamic models using Volterra polynomials. Models based on the Volterra theory are used to describe stochastic systems [8], as well as for the structural identification of nonlinear dynamic systems [9]. A systematic approach to modeling nonlinear dynamic systems by formalizing the relationship between input $x(t)$ and output $y(t)$ was first implemented by Norbert Wiener [10]. He applied the Volterra series in the analysis of nonlinear electronic circuits. He developed efficient identification algorithms for the case of an input signal in the form of Gaussian white noise. Wiener's research was continued in the works of Marmarelis, Schetzen, Rugh, and other researchers (see, for example, the reviews in [11,12]). The system responses to test signals in the form of ideal white noise are used to identify the Wiener kernels. In practice, the implementation of such input actions is carried out with inevitable errors, which are compensated by choosing the optimal range in test disturbances [13]. When solving inverse quantum mechanical problems, researchers use wave functions [14] to construct Volterra integral models. The identification of Volterra kernels is based on minimizing the root-mean-square error from the response of the dynamic system tested. This approach is associated with the extreme complexity of practical implementation [15].

In this regard, they strive to achieve a simplification of the methods (see, for example, [16–19]). In particular, the authors of [18] implemented the case where Volterra kernels are assumed to be separable,

$$K_i(s_1,\ldots,s_i) = \prod_{n=1}^{i} g(s_n), i = \overline{1,3}, \tag{2}$$

as well as the satisfiability of a priori conditions,

$$K_n(s_1,\ldots,s_n) = 0, n > 3. \tag{3}$$

Reference [16] considered a modified discrete analog of the cubic Volterra polynomial.

$$\begin{aligned} y(t_i) = &\sum_{m_1=0}^{N_1-1} K_1(t_{m_1})x(t_{i-m_1}) + \sum_{m_1=0}^{N_2-1}\sum_{m_2=m_1}^{N_2-1} K_2(t_{m_1},t_{m_2})x(t_{i-m_1})x(t_{i-m_2}) + \\ &+ \sum_{m_1=0}^{N_3-1}\sum_{m_2=m_1}^{N_3-1}\sum_{m_3=m_2}^{N_3-1} K_3(t_{m_1},t_{m_2},t_{m_3})x(t_{i-m_1})x(t_{i-m_2})x(t_{i-m_3}), \end{aligned} \tag{4}$$

where the symmetric kernels K_2 and K_3 are defined only on one of the subdomains $0 \le m_1 \le m_2 \le N_2 - 1$ and $0 \le m_1 \le m_2 \le m_3 \le N_3 - 1$, respectively. To reduce computational costs, the authors of [16] proposed a transition from (4) to relations

$$y(t_i) = \sum_{m_1=0}^{N_1-1} K_1(t_{m_1})x(t_{i-m_1}) + \sum_{m_1=0}^{N_2-1}\sum_{m_2=m_1}^{N_2-1} K_2(t_{m_1},t_{m_2})x(t_{i-m_1})x(t_{i-m_2}) + \sum_{m=0}^{N_3-1} \widetilde{K}_3(t_m)x^3(t_{i-m}) \tag{5}$$

or

$$y(t_i) = \sum_{m_1=0}^{N_1-1} K_1(t_{m_1})x(t_{i-m_1}) + \sum_{m=0}^{N_2-1} \widetilde{K}_2(t_m)x^2(t_{i-m}) + \sum_{m=0}^{N_3-1} \widetilde{K}_3(t_m)x^3(t_{i-m}). \tag{6}$$

It depends on the statistical properties of the input signals. In this case, they solve the problem of restoring the functions $\widetilde{K}_n$ of one variable instead of the problem of determining in (4) the functions K_n, $n = 2,3$, of many variables in (5) and (6). Moreover, instead of searching for $K_n(t, s_1,\ldots,s_n)$ on the entire domain of definition $0 \le s_1,\ldots,s_n \le t \le T$, researchers confine themselves to the values of the function at fixed values $s_1 = s_2 = \ldots = s_n = t$, $t \in [0,T]$. In particular, this approach was applied in [20] (p. 1387) and [21] (p. 1078). The critical review of [22] (pp. 178–179) explained the difference between these problems in detail using the approaches described in [23,24] as an example.

As noted in [25], "for the presentation of information in the time domain, the expediency of using pulsed and stepped test signals is obvious". A method based on the

δ-functions use was proposed in [26] and developed later in [27]. It suggests using the $(n-1)$-parametric family,

$$x_{\omega_1,\ldots,\omega_{n-1}}(t) = \sum_{j=0}^{n-1} \delta\big(t-\omega_j\big), \omega_0 = 0, \omega_j \geq 0, \sum_{j=0}^{n-1} \omega_j \leq t \leq T, \tag{7}$$

where $\delta(s)$ is the Dirac δ-function,

$$\delta(s) = \begin{cases} 0, s \neq 0, \\ \infty, s = 0, \end{cases}$$

as test actions for identifying the $K_n(s_1,\ldots,s_n)$.

A discrete analog of this approach is the numerical algorithm proposed in [28]. Note that the technique based on (6) has a limited scope. An explanation for this can be found in [29] (p. 142): " … this simple idea is impulse-response analysis. Its basic weakness is that many physical processes do not allow pulse inputs … Moreover, such input could make the system exhibit nonlinear effect that would disturb the linearized behavior we have set out to model". Readers can find a detailed review of identification methods based on impulse disturbances [27,30].

Let us now turn to methods based on the application of Heaviside functions $e(t)$. Reference [31] considered an approach related to approximating on $[0,T]$ a periodic test signal by discretely given stepwise one with a constant quantization step. It is assumed the initial continuous input signal has a constant period T. This technique was further developed in [32,33], in which

$$x_{\omega_1,\ldots,\omega_{n-1}}(t) = \sum_{j=1}^{n} C_{\omega_j} \alpha e\big(t-\omega_j\big), \omega_j \geq 0, \sum_{j=1}^{n} \omega_j \leq t \leq T,$$

was used as the test signal for identifying $K_n, n \geq 2$, where α is the signal amplitude (height), and C_{ω_j} is a logical variable equal to zero if

$$\omega_j = 0.$$

In [34], a modification was made for a dynamical system with two inputs. Here, the identification process included a heuristic algorithm for dividing the system response $y(t)$ into components due to the influence of a separate integral term of the quadratic Volterra model.

In this paper, we consider dynamic systems, the transient characteristics of which are presented in the time domain. The possibility of scaling in time makes it possible to study fast processes that are typical for many technical (energy) systems. The method of finding the transient characteristics of the system is deterministic. Fewer data are required to formalize the mathematical model in comparison with the probabilistic method. The collection of initial data occurs during the execution of an active experiment, which implies the possibility of influencing the system with test input signals. In comparison with a passive experiment (observation), this method allows one to reduce the time for collecting initial data and specify the type of test signal.

Reference [3] presented a method for identifying Volterra kernels using a combination of Heaviside functions with a deviating argument as test signals. Its advantage lies in the transition from the original problem to the solution of such special multidimensional Volterra equations of the first kind with variable upper and lower integration limits, which have explicit inversion formulas. The scope of this technique for modeling the dynamics of real-life technical objects is limited by the complexity of the formation of piecewise constant test signals. Reference [35] considered the possibility of using test signals of a piecewise linear form,

$$x(t) \equiv x_\nu(t) = \begin{cases} 0, & t \le 0, \\ \frac{t}{\nu}, & 0 < t \le \nu, \\ 1, & t > \nu, \end{cases} \tag{8}$$

in the problem of identifying a two-dimensional continuum of unknowns from a linear Volterra equation of the first kind with a nonstationary kernel. Figure 1 shows the form of the input signal (8).

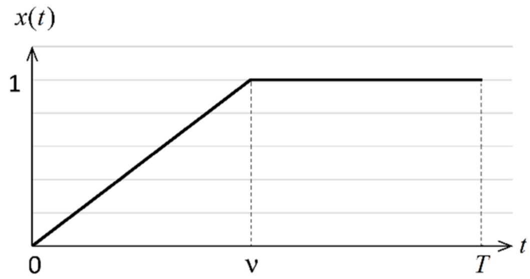

Figure 1. The form of the input signal (8).

The chosen modification of the input signals simplifies their formation in practice, and the distinguished Volterra integral equations of the first kind, as before, have a unique solution in the class of continuous functions.

The identification method was developed to further apply it for numerical modeling the process of automatic simulation of the nonlinear dynamics of heat and electric power industry objects based on Volterra polynomials with a vector input.

The purpose of this work is, firstly, to use the reserve for increasing the accuracy of constructing an integral model, presented as a modified quadratic Volterra polynomial, through the use of piecewise linear signals close to real-life dynamic systems, and secondly, to develop measurement noise-resistant algorithms for identifying functions two variables.

The paper is organized as follows: Section 2 describes the technique for building an integral model using piecewise linear test signals. It also presents an example illustrating the effect of increasing the accuracy of modeling the linear term by applying piecewise linear signals. Section 3 contains a numerical algorithm for identifying the quadratic term of the Volterra series based on smoothing cubic splines. Section 4 considers the implementation of the numerical solution algorithm using the quadrature method. Section 5 suggests directions for future work. Section 6 contains the main results.

2. Method for Constructing a Quadratic Volterra Polynomial

Let us consider a quadratic model containing a linear nonstationary component,

$$y(t) = \int_0^t K_1(t,s)x(s)ds + \int_0^t \int_0^t K_2(s_1,s_2)x(t-s_1)x(t-s_2)ds_1 ds_2, t \in [0,T]. \tag{9}$$

To identify the Volterra kernels $K_1(t,s)$, $0 \le s \le t \le T$, $K_2(s_1,s_2)$, $0 \le s_1, s_2 \le t \le T$, the authors of [36] used test signals

$$x(t) \equiv x_\nu^{\alpha_{1,2}}(t) = \alpha_{1,2}(e(t) - e(t-\nu)), 0 \le \nu \le t \le T, \tag{10}$$

where $\alpha_1 \neq \alpha_2$. Figure 2 shows the form of the input signal (10) when the signal amplitude is equal to 1.

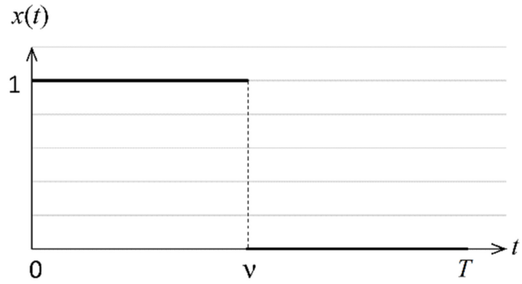

Figure 2. The form of the input signal (10).

Substituting (10) in (9) leads to the following system:

$$\begin{array}{l}\alpha_1 \int\limits_0^{\nu} K_1(t,s)ds + \alpha_1^2 \int\limits_{t-\nu}^{t} \int\limits_{t-\nu}^{t} K_2(s_1,s_2)ds_1 ds_2 = y^{\alpha_1}(t,\nu), \\ \alpha_2 \int\limits_0^{\nu} K_1(t,s)ds + \alpha_2^2 \int\limits_{t-\nu}^{t} \int\limits_{t-\nu}^{t} K_2(s_1,s_2)ds_1 ds_2 = y^{\alpha_2}(t,\nu),\end{array} \tag{11}$$

where $\alpha_1 \neq \alpha_2$, $0 \leq \nu \leq t \leq T$, which implies that

$$K_1(t,\nu) = f'_{1\nu}(t,\nu), \tag{12}$$

$$K_2(t,t-\nu) = \frac{1}{2}\Big(f''_{2t\nu}(t,\nu) + f''_{2\nu^2}(t,\nu)\Big), \tag{13}$$

where

$$f_1(t,\nu) = \frac{\alpha_2^2 y^{\alpha_1}(t,\nu) - \alpha_1^2 y^{\alpha_2}(t,\nu)}{\alpha_1\alpha_2(\alpha_2-\alpha_1)}, \tag{14}$$

$$f_2(t,\nu) = \frac{\alpha_1 y^{\alpha_2}(t,\nu) - \alpha_2 y^{\alpha_1}(t,\nu)}{\alpha_1\alpha_2(\alpha_2-\alpha_1)}. \tag{15}$$

Let us carry out the procedure for identifying the Volterra kernel $K_2(s_1,s_2)$ symmetric in variables s_1, s_2, using Equations (13) and (15). Then the problem of identifying $K_1(t,s)$ from (9) reduces to solving

$$\begin{array}{c}\int\limits_0^t K_1(t,s)x(s)ds = q(t), \\ q(t) = y(t) - \int\limits_0^t \int\limits_0^t K_2(s_1,s_2)x(t-s_1)x(t-s_2)ds_1 ds_2,\end{array} \tag{16}$$

where $K_2(s_1,s_2)$ is known. Applying test signals (8) in addition to (10), we obtain Equation (16), where

$$q(t) \equiv q_\nu(t) = \begin{cases} 0, & t = 0,\ \nu = 0, \\ g(t,\nu), & 0 < \nu \leq t, \end{cases}$$

which can be represented in the form

$$\int\limits_0^{\nu} K_1(t,s)\frac{s}{\nu}ds + \int\limits_{\nu}^{t} K_1(t,s)ds = q(t,\nu), \tag{17}$$

$$\begin{array}{c}q(t,\nu) = g(t,\nu) - \int\limits_{t-\nu}^{t} \int\limits_{t-\nu}^{t} K_2(s_1,s_2)\frac{t-s_1}{\nu}\frac{t-s_2}{\nu}ds_1 ds_2 - \\ -2\int\limits_{t-\nu}^{t} ds_1 \int\limits_0^{t-\nu} K_2(s_1,s_2)\frac{t-s_2}{\nu}ds_2 - \int\limits_0^{t-\nu} \int\limits_0^{t-\nu} K_2(s_1,s_2)ds_1 ds_2.\end{array}$$

Here, $g(t,\nu)$ is the response of a dynamic object to a signal (8) at $0 \le \nu \le t \le T$. Following [35,37], the inversion Formula (17) has the form

$$K_1(t,\nu) = -\left(2g'_{\nu}(t,\nu) + \nu g''_{\nu^2}(t,\nu)\right). \tag{18}$$

Let us compare the effect of using test signals (8) and (10) when building an integral model (9).

The below example demonstrates the effect of increasing the simulation accuracy when using test signals of the form (8). Let the "reference" dynamical system be represented by a cubic Volterra polynomial with kernels $K_1 = 1$, $K_2 = \frac{1}{2}$, $K_3 = \frac{1}{3!}$, so that

$$y_{et}(t) = \int_0^t x(s)ds + \frac{1}{2}\left(\int_0^t x(s)ds\right)^2 + \frac{1}{3!}\left(\int_0^t x(s)ds\right)^3. \tag{19}$$

The technique for constructing quadratic and cubic Volterra polynomials, based on the use of piecewise constant test signals of type (10), has been successfully tested on dynamic systems of various physical nature, including a mathematical model of type (19), as well as in modeling the dynamics of a heat exchanger element and wind power plant [38]. Note that (19) is a partial sum of the series for the function

$$e^{\int_0^t x(s)ds} - 1.$$

This function has proven itself well in the study of the areas of applicability of identification algorithms for quadratic and cubic Volterra polynomials [38,39]. We apply the procedure for identifying kernels by using test signals (10) with amplitudes $\alpha_1 = -\alpha_2 = \alpha > 0$ and, instead of (9), obtain

$$y_1(t) = \int_0^t \left(1 + \frac{\alpha^2}{2}s^2\right)x(s)ds + \frac{1}{2}\left(\int_0^t x(t-s)ds\right)^2, \tag{20}$$

where the Volterra kernels were restored using Equations (12) and (13), respectively.

The combined model (9) with the addition to (10) test signals (8) with amplitude α for identification $K_1(t,s)$ has the form

$$y_2(t) = \int_0^t \left(1 + \alpha^2\left(\frac{1}{4}s^2 - \frac{3}{4}ts + \frac{1}{2}t^2\right)\right)x(s)ds + \frac{1}{2}\left(\int_0^t x(t-s)ds\right)^2, \tag{21}$$

where the kernel identification was performed using Equations (18) and (13), respectively. On signals $x^{\beta}(t) = \frac{t}{\beta}$, $\beta = k \cdot \alpha \cdot 0.01$, $k = \overline{1,B}$, model (20) gives residual

$$n_1(t) = y^{\beta}_{et}(t) - y^{\beta}_1(t) = \frac{t^6}{48\beta^3} - \frac{\alpha^2 t^4}{8\beta},$$

and model (21) gives residual

$$n_2(t) = y^{\beta}_{et}(t) - y^{\beta}_2(t) = \frac{t^6}{48\beta^3} - \frac{\alpha^2 t^4}{16\beta},$$

where y^{β}_{et} is the response (19) to signal $x^{\beta}(t)$.

Let us present an algorithm for constructing the polynomial (9) for modeling the response of the dynamic system represented in the form (19).

Step 1. Calculation of the values of $y^{\alpha}_{et}(t,\nu)$ and $y^{-\alpha}_{et}(t,\nu)$ using substitution (10) with amplitude $\alpha_1 = -\alpha_2 = \alpha > 0$ into the right-hand side of (19).

Step 2. Calculation by (15) of the values of the right-hand side of the integral equation,

$$\int\limits_{t-\nu}^{t}\int\limits_{t-\nu}^{t} K_2(s_1,s_2)ds_1ds_2 = f_2(t,\nu)\ ,0 \le \nu \le t \le T.$$

Step 3. Application of Equation (13) for identifying $K_2(s_1,s_2)$, $0 \le s_1, s_2 \le T$.

Step 4. Calculation of values $y^{\alpha}_{et}(t,\nu)$ using substitution (8) with an amplitude α into the right-hand side of (19).

Step 5. Calculation of the right-hand side of (17) $q(t,\nu)$, where $K_2(s_1,s_2)$ and $q(t,\nu) \equiv y^{\alpha}_{et}(t,\nu)$ are obtained in the previous steps 3 and 4, respectively.

Step 6. Application of Equation (18) for identifying $K_1(t,\nu)$, $0 \le \nu \le t \le T$.

Step 7. Substitution of kernels $K_2(s_1,s_2)$ and $K_1(t,\nu)$ obtained in steps 3 and 6, respectively, into the right-hand side of (9). This leads to (21).

Modeling accuracy $y_1(t)$ was compared with response $y_2(t)$. The value of the "mean absolute error" coefficient was chosen as a criterion for modeling accuracy.

$$MAE_r(t) = \frac{1}{B}\sum_{\beta=1}^{B}|n_r(t)|,\ r = 1,2,\ t \in [0,15].$$

In Figure 3, black color shows the areas of fulfillment of the inequality $MAE_2(t) < MAE_1(t)$ for $B = 10, 25, 40$ with an accuracy of $\delta = 10^{-2}$.

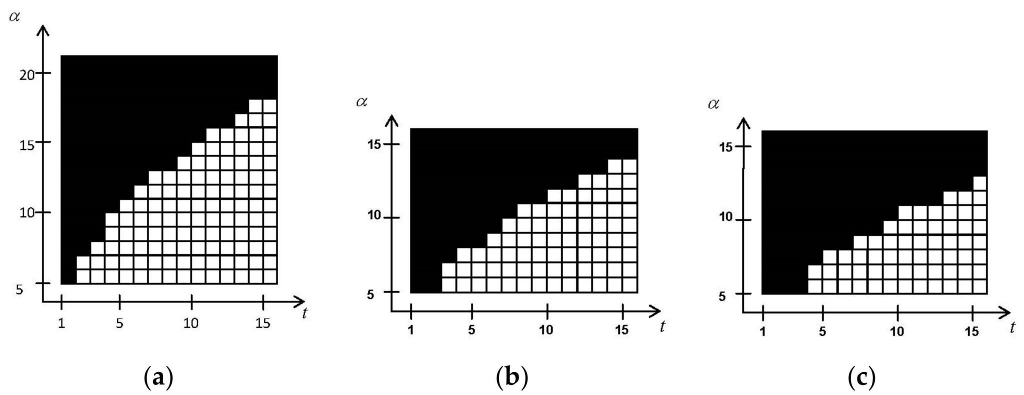

Figure 3. Areas of fulfillment of the inequality $MAE_2(t) < MAE_1(t)$ for (**a**) $B = 10$, (**b**) $B = 25$, and (**c**) $B = 40$.

The computational experiment showed that the areas of efficiency of the integral models (20) and (21) depend on the length of the segment T, the amplitude of the test signals α used to identify the Volterra kernels, and the accuracy of the calculations δ.

Note that we assumed the quadratic term, the two-dimensional kernel $K_2(t,\nu)$, in Equation (18) to be known. Therefore, in the next section, we consider an algorithm for identifying this term using Equation (13).

3. Identification Algorithm for Quadratic Term

Unfortunately, the implementation of the obtained inversion Equation (13) in practice faces a fundamental difficulty: the differentiation operation is an ill-posed one [40]. One of the manifestations of ill-posedness is large errors in calculating the derivative, even for very small errors in specifying a differentiable function. Note that the operation of subtraction in (15) of the registration errors of two functions leads to an increase in the variance of the total error in setting the function $f_2(t,\nu)$. Thus, stable differentiation of noisy data becomes an urgent problem for the implementation of formula (13) in practice.

Reference [41] constructed a stable identification algorithm on the basis of Equation (12) (a stable identification algorithm is an algorithm in which the relative identification error is comparable to the relative error of the initial data). There, a smoothing cubic spline (SCS) of a defect unit was used for a stable calculation of the first derivative. The smoothing parameter was chosen from the condition of the minimum root-mean-square smoothing error. The use of smoothing splines becomes much more complicated in the case of identifying the quadratic kernel $K_2(\tau, s)$. First, to calculate the second-order mixed derivative $f''_{2t\nu}(t, \nu)$, we need to build a smoothing bicubic spline (SBS), which is a function of two variables t, ν. Secondly, the boundary conditions are now given not at two extreme points of the SCS construction interval, but on four straight lines, which are the boundaries of the rectangular area of the SCS construction. Thirdly, due to the different "smoothness" of the function $f_2(t, \nu)$ in different variables, we now have to choose two smoothing parameters from the condition for the minimum smoothing error. These difficulties caused the main problems that were not solved in the corresponding scientific publications and which are addressed in this section.

Suppose that the values of the function $f_2(t, \nu)$ are determined at the nodes of a rectangular grid. To take into account possible errors (noise) of measurements, the following representation of noisy measurements $\tilde{f}_2(t_i, \nu_j)$ is taken:

$$\tilde{f}_2(t_i, \nu_j) = f_2(t_i, \nu_j) + \eta_{i,j},\ i = 1, \ldots, N_t, j = 1, \ldots, N_\nu,$$

where $\eta_{i,j}$ is random measurement noise with zero mean value and variance σ_η^2 (equally accurate measurements). Note that nodes t_i and ν_j may not have the same or equal steps. It is required to calculate the values of derivatives $f''_{2t\nu}(t, \nu)$, $f''_{2\nu^2}(t, \nu)$ at the given nodes from the initial data $\left\{\tilde{f}_2(t_i, \nu_j)\right\}$.

For a stable calculation of these derivatives, we turn to SCS [42] widely used in the processing of experimental data [43,44]. Suppose we have N_ν nodes $V_1 = \nu_1 < \nu_2 < \ldots < \nu_{N_\nu} = V_2$ at some interval $[V_1, V_2]$. In these nodes, the values of the function (signal) $f(\nu)$ are measured as follows:

$$\tilde{f}_j = f(\nu_j) + \eta_j, j = 1 \ldots N_\nu, \tag{22}$$

where η_j is the random measurement noise with zero mean and variance σ_η^2 (equally accurate measurements). The smoothing cubic spline $S_{N_\nu,\alpha}(\nu)$ of a defect unit on each segment $[\nu_j, \nu_{j+1})$ can be represented by a cubic polynomial of the following form [42]:

$$S_{N_\nu,\alpha}(\nu) = a_j + b_j \cdot (\nu - \nu_j) + c_j \cdot (\nu - \nu_j)^2 + d_j \cdot (\nu - \nu_j)^3. \tag{23}$$

Moreover, the function $S_{N_\nu,\alpha}(\nu)$ must be twice continuously differentiable on the entire interval $[V_1, V_2]$ of its definition. Note that, in contrast to the interpolation spline (passing through the points $\left(\nu_j, \tilde{f}_j\right)$), the smoothing cubic spline $S_{N_\nu,\alpha}(\nu)$ generally does not pass through these points, but passes more "smoothly" in some neighborhoods of these points (depending on the smoothing parameter α), thereby providing smoothing (filtering) of measurement noise.

To uniquely calculate the spline coefficients a_j, b_j, c_j, d_j, boundary conditions are set at the nodes ν_1, ν_{N_ν}. The following conditions are most often used [42,44]:

- conditions on zero second derivatives of the spline (natural boundary conditions),

$$S''_{N_\nu,\alpha}(\nu_1) = 0;\ \ S''_{N_\nu,\alpha}(\nu_{N_\nu}) = 0, \tag{24}$$

- conditions on the first derivatives of the spline,

$$S'_{N_\nu,\alpha}(\nu_1) = s'_1;\ \ S'_{N_\nu,\alpha}(\nu_{N_\nu}) = s'_{N_\nu}, \tag{25}$$

as well as a combination of these conditions (for example, condition (25) is on the left, condition (24) is on the right). It was shown [42] the SCS constructed under these conditions provides a minimum to the functional

$$F_\alpha(S) = \alpha \cdot \int\limits_{\nu_1}^{\nu_{N_\nu}} |S''(\nu)|^2 d\nu + \sum_{j=1}^{N_\nu} p_j^{-1} \cdot (\widetilde{f}_j - S(\nu_j))^2, \quad (26)$$

where p_j denotes the weight factors reflecting the accuracy of the j-th measurement $\widetilde{f}_j$ (they are given the same in the case of equally accurate measurements).

To calculate the spline coefficients (for a given smoothing parameter), it is necessary to compose a system of linear algebraic equations with a five-diagonal matrix concerning some vector (as a rule, these are the values of the second derivative of the spline at the nodes $\{\nu_j\}$), through which all the spline coefficients are then found (for details, see [42,44]).

The smoothing parameter α "controls" the smoothness of the spline, and the smoothing error (as well as the differentiation error) depends significantly on the value of this parameter [44,45]. There is a parameter value (let us call it optimal) for which the smoothing error (in the accepted norm) is minimal [45]. Let us temporarily assume that we have found an acceptable (in terms of the minimum smoothing error) value of the smoothing parameter (the choice of the parameter is discussed in the next section).

Remark 1. *It follows from the form of the integrals (11) that the function $f_2(t,\nu)$ takes nonzero values for the arguments satisfying the condition $\nu \le t$. For other values of ν, t, the function is equal to zero due to the condition of the technical feasibility of the system with negative values of the arguments, i.e., $k_2(t,\nu) \equiv 0$, if $\nu < 0$, $t < 0$.*

To eliminate the discontinuity of the first kind at $\nu = t$ values when constructing a smoothing spline, we propose to supplement the values of the function $f_2(t,\nu)$ for $\nu > t$ according to the following rule:

$$f_2(t, t+\Delta\nu) = \begin{cases} 2f_2(t,t) - f_2(t, t-\Delta\nu), & 0\Delta\nu \le t; \\ 2f_2(t,t), & t\Delta\nu \le T - t. \end{cases}$$

We denote the function supplemented in this way as $f_2^*(t,\nu)$.

Initially, we focus on the algorithm for calculating the values of the derivative $f''_{2\nu^2}(t,\nu)$. It can be represented by the following steps:

Step 1. We set the boundary conditions, the combination of which at the extreme points ν_1, ν_{N_ν} of the construction interval is determined on the basis of available a priori information about the function $f_2^*(t,\nu)$. If such reliable information is not available, then one should turn to the natural boundary conditions (24).

Step 2. For each $i = 1,\ldots,N_t$, we form a dataset

$$\left\{\nu_j, \widetilde{f}1_j^{(i)} = \widetilde{f}_2^*(t_i,\nu_j), j = 1,\ldots,N_\nu\right\},$$

select the smoothing parameter $\alpha1^{(i)}$, and build the SCS $S1^{(i)}_{N_\nu,\alpha1^{(i)}}(\nu)$, from which we then calculate the first derivative $\hat{f}'_{2\nu}(t_i,\nu_j) = \frac{d}{d\nu}S1^{(i)}_{N_\nu,\alpha1^{(i)}}(\nu)|_{\nu=\nu_j} = b1_j^{(i)}$ (an estimate of the derivative $f'_{2\nu}(t_i,\nu_j)$), where $b1_j^{(i)}$ is the coefficient of spline $S1^{(i)}_{N_\nu,\alpha1^{(i)}}(\nu)$ in representation (23).

Step 3. For each Y, we again form the dataset

$$\left\{\nu_j, \widetilde{f}2_j^{(i)} = \hat{f}'_{2\nu}(t_i,\nu_j), j = 1,\ldots,N_\nu\right\},$$

select the smoothing parameter $\alpha 2^{(i)}$, and build the SCS $S2^{(i)}_{N_\nu,\alpha 2^{(i)}}(\nu)$, the first derivative of which is the estimate $\hat{f}''_{2\nu^2}(t_i,\nu_j) = \frac{d}{d\nu} S2^{(i)}_{N_\nu,\alpha 2^{(i)}}(\nu)|_{\nu=\nu_j} = b2^{(i)}_j$ for the second derivative $f''_{2\nu^2}(t_i,\nu_j)$, where $b2^{(i)}_j$ is the coefficient of spline $S2^{(i)}_{N_\nu,\alpha 2^{(i)}}(\nu)$ in representation (23).

Thus, we calculate estimates of the second derivative $f''_{2\nu^2}(t_i,\nu_j)$ for t_i, $i = 1,\ldots,N_t$.

Let us proceed to the construction (following the technique of [46]) of a bicubic smoothing spline for calculating the mixed derivative $f''_{2t\nu}(t_i,\nu_j)$. We use the following algorithm:

Step 1. For each $j = 1,\ldots,N_\nu$, we again form a dataset (fix the value of ν_j)

$$\left\{t_i, \widetilde{f}3^{(j)}_i = \widetilde{f}^*_2(t_i,\nu_j), i = 1,\ldots,N_t\right\},$$

select the smoothing parameter $\alpha 3^{(j)}$, build the SCS $S3^{(j)}_{N_t,\alpha 3^{(j)}}(t)$, from which we then calculate the first derivative $\hat{f}'_{2t}(t_i,\nu_j) = \frac{d}{dt} S3^{(j)}_{N_t,\alpha 3^{(j)}}(t)|_{t=t_i} = b3^{(j)}_i$ (estimation of the derivative $f'_{2t}(t_i,\nu_j)$), where $b3^{(j)}_i$ is the coefficient of spline $S3^{(j)}_{N_t,\alpha 3^{(j)}}(t)$ in representation (23).

Step 2. For each Y, we form a dataset

$$\left\{\nu_j, \widetilde{f}4^{(i)}_j = \hat{f}'_{2t}(t_i,\nu_j), j = 1,\ldots,N_\nu\right\},$$

select a smoothing parameter $\alpha 4^{(i)}$, build an SCS $S4^{(i)}_{N_\nu,\alpha 4^{(i)}}(\nu)$, the first derivative of which is an estimate $\hat{f}''_{2t\nu}(t_i,\nu_j) = \frac{d}{d\nu} S4^{(i)}_{N_\nu,\alpha 4^{(i)}}(\nu)|_{\nu=\nu_j} = b4^{(i)}_j$ for the mixed derivative $f''_{2t\nu}(t_i,\nu_j)$, where $b4^{(i)}_j$ is the coefficient of spline $S4^{(i)}_{N_\nu,\alpha 4^{(i)}}(\nu)$ in representation (23).

Thus, we repeat step 1 for $\nu_j, j = 1,\ldots,N_\nu$, and step 2 for $t_i, i = 1,\ldots,N_t$. After calculating the estimates $\hat{f}''_{2\nu^2}(t_i,\nu_j)$, $\hat{f}''_{2t\nu}(t_i,\nu_j)$ using Equation (13), we find the estimate $\hat{k}_2(t_i - \nu_j, t_i)$ for the values $\nu_j \le t_i$.

Remark 2. *The inversion Equation (13) determines the value of the quadratic kernel $K_2(t,\nu)$ for the arguments $0 \le \nu \le t \le T$, i.e., for the values of the argument $\nu \le t$. The line $\nu = t$ is the axis of symmetry of the kernel $K_2(t,\nu)$ (follows from the one-dimensionality of the input signal); therefore, to determine the values of the kernel for $\nu = t + \Delta\nu > t$, where $\Delta\nu > 0$, we propose a symmetrical supplement of the kernel values according to the formula $K_2(t, t+\Delta\nu) = K_2(t+\Delta\nu, t)$.*

Remark 3. *Since the construction of the SCS by the variable ν requires approximately $C_{oper} \cdot N_\nu$ arithmetic operations, where $C_{oper} \approx 30$ [42], the proposed algorithm for calculating derivatives requires approximately $C^4_{oper} \cdot N^3_\nu \cdot N_t$ operations. Therefore, the proposed algorithms for calculating derivatives have a high computational efficiency even with a large dimension of the grid (t_i,ν_j).*

Previously, the values of the smoothing parameters $\alpha 1^{(i)}$, $\alpha 2^{(i)}$, $\alpha 3^{(j)}$, $\alpha 4^{(i)}$ selected were assumed (i.e., determined). Therefore, the question of how to choose these parameters arises, which will significantly affect the error of smoothing and differentiation. If the variance σ^2_η of the measurement noise (see (22)) were reliably known (at least with an accuracy of 5–8%), then the selection algorithm constructed on the basis of checking the optimality criterion of the linear filtering algorithm would allow, with acceptable accuracy (5–8%), to estimate the values of the optimal smoothing parameter that minimizes the value of the root-mean-square smoothing error (see [44] (pp. 60–67), [45]). It is obvious that the situation with unknown noise dispersion is most characteristic in solving practical identification problems. Therefore, to choose a parameter in this case, we turn to the L-curve method used to choose the regularization parameter in algorithms for solving linear ill-posed problems (for example, [47,48]). In [49], a modification of the L-curve method was proposed for choosing the smoothing parameter.

Let us talk briefly about the essence of this selection algorithm. Let us introduce the following functionals (see [49]):

$$\rho(\alpha) = \sum_{j=1}^{N_\nu} p_i^{-1} \cdot \left(\widetilde{f}_j - S_{n,\alpha}(\nu_j)\right)^2, \ \gamma(\alpha) = \int_{\nu_1}^{\nu_{N_\nu}} \left| S''_{N_\nu,\alpha}(\nu) \right|^2 d\nu.$$

Then, an L-curve (whose shape resembles the outline of the Latin letter L) is a parametric curve with coordinates $(\rho(\alpha), \gamma(\alpha))$. It can be shown that the curvature of an L-curve is given by the following formula:

$$k_L(\alpha) = 2 \cdot \frac{\hat{\rho}'(\alpha) \cdot \hat{\gamma}''(\alpha) - \hat{\rho}''(\alpha) \cdot \hat{\gamma}'(\alpha)}{\left[(\hat{\rho}'(\alpha))^2 + \left(\hat{\gamma}'(\alpha)\right)^2 \right]^{\frac{3}{2}}}, \tag{27}$$

where $\hat{\rho}(\alpha) = \ln \rho(\alpha)$, $\hat{\gamma}(\alpha) = \ln \gamma(\alpha)$. The smoothing parameter is the value α_L for which the curvature $k_L(\alpha)$ takes on the maximum value. To effectively calculate the value of the functional $\gamma(\alpha)$, the following formula is proposed:

$$\gamma(\alpha) = \sum_{i=1}^{n-1} \left(4c_i^2 \cdot h_i + 12c_i \cdot d_i \cdot h_i^2 + 12d_i^2 \cdot h_i^3 \right),$$

where $h_i = t_{i+1} - t_i, i = 1, \ldots, n-1$, c_i, d_i are the SCS coefficients in representation (23), calculated for a given parameter α. To calculate the curvature value using Equation (27), an approach is proposed that uses cubic interpolation splines to approximate the dependences $\hat{\rho}(\alpha)$, $\hat{\gamma}(\alpha)$ (for details, see [49]). An extensive computational experiment was also carried out there to answer the following question: Is the loss due to smoothing error large when α_L is used instead of the optimal α_{opt} (which can only be determined in a computational experiment)? The experiment was carried out with functions that are "typical" output signals of a dynamic system when step signals are applied to the input. The analysis of the results of the experiment showed that the algorithm for selecting the smoothing parameter on the basis of the L-curve method makes it possible to estimate the optimal value of the smoothing parameter quite well. The increase in the smoothing error when using the parameter α_L does not exceed 5–15% on average compared to α_{opt}, the calculation of which is impossible in practice. Therefore, to calculate the smoothing parameters $\alpha 1^{(i)}$, $\alpha 2^{(i)}$, $\alpha 3^{(j)}$, and $\alpha 4^{(i)}$, it is proposed to use the described algorithm for choosing the smoothing parameter on the basis of the L-curve method.

To test the proposed algorithm of identifying quadratic kernel, a numerical experiment was carried out, some of the results of which we present in this paper. The test quadratic kernel $K_2(\tau, s)$ is a function used to describe the dynamics of some type of heat exchangers [50]. Figure 4a shows the surface of this function, and Figure 4b shows isolines. The time interval boundary was $T = 1$, while the number of nodes was $N_t = 80$, $N_\nu = 80$.

First, we define the methodological error of the identification algorithm. To do this, we calculated the values of the function (15) at the nodes $t_i, i = 1, \ldots, N_t$, $\nu_j, j = 1, \ldots, N_\nu$, which were interpreted as the exact values of the function $f_2(t_i, \nu_j)$. These data, presented as a matrix F with dimensions 80×80 with elements $F_{i,j} = f_2(t_i, \nu_j)$, were the initial data for the proposed identification algorithm. Since these initial data were taken as exact, instead of SCS, we built interpolating cubic splines (including the bicubic spline) with boundary conditions (24). We calculated estimates for the derivatives $\hat{f}''_{2\nu^2}(t_i, \nu_j)$ and $\hat{f}''_{2t\nu}(t_i, \nu_j)$ on the basis of these splines and then constructed an estimate for the quadratic kernel using Equation (9) (see Remark 2). Figure 5 shows the isolines of this estimate, having a relative identification error $\delta_K = \frac{\|K_2 - \hat{K}_2\|}{\|K_2\|} = 0.011$, where K_2, $\hat{K}_2$ are matrices composed of the values of the exact kernel $K_2(t_i, \nu_j)$ and its estimates $\hat{K}_2(t_i, \nu_j)$, respectively, and $\|\cdot\|$ is the Euclidean norm of the matrix. Approximately the same error was observed for other grid sizes in t, ν. Therefore, we can conclude the proposed identification algorithm has a low methodological error.

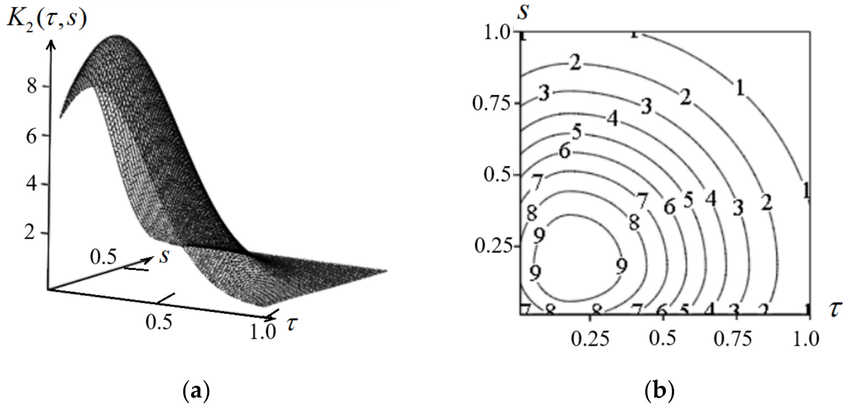

Figure 4. Test quadratic kernel: (**a**) the surface of $K_2(\tau, s)$; (**b**) isolines.

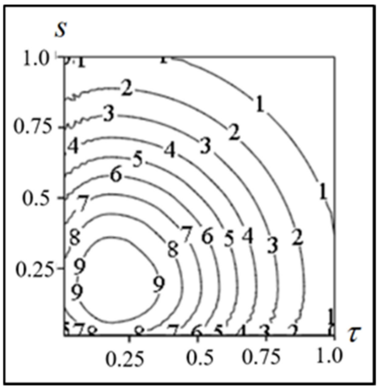

Figure 5. Estimation of the kernel $\hat{K}_2(\tau, s)$, built on exact data.

Let us consider the influence of the measurement noise of the function $f_2(t, \nu)$ on the accuracy of identification. To do this, we distorted all elements of the "exact" matrix F with normally distributed noise with a relative level $\delta_F = \frac{\|F - \widetilde{F}\|}{\|F\|}$, where $\widetilde{F}$ is a matrix with "noisy" elements. The matrix $\widetilde{F}$ thus formed was used as initial data for the previously described identification algorithm. We chose the smoothing parameter at all steps of calculating derivatives using the L-curve method described above. Figure 6 shows the isolines of the estimate $\hat{K}_2(t_i, \nu_j)$, built at a noise level of 0.02. The relative identification error was $\delta_K = 0.044$, which indicates the acceptable accuracy of quadratic term identification by the proposed algorithm.

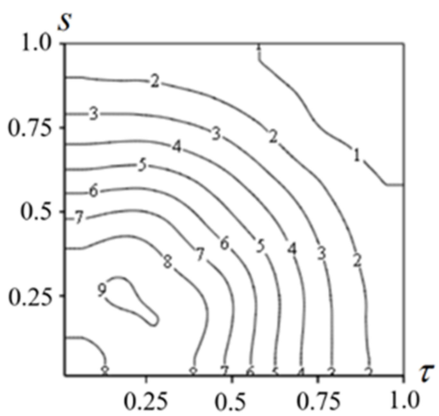

Figure 6. Estimation of the kernel $\hat{K}_2(\tau, s)$, built on noisy data.

4. Difference Scheme for Finding a Linear Nonstationary Kernel Using the Quadrature Method

It often happens in practice that the responses of the system (the right-hand side of equations) are given not analytically, but in the form of a series of numbers. In this case, we have to turn to the numerical solution. The procedure for the numerical identification of the Volterra polynomial (9) using piecewise constant test signals (10) was considered in detail earlier in [36]. This approach to constructing a quadratic polynomial was tested in applications for thermal power objects [51]. As shown in the previous section, using signals of a new type with a rising edge of the form (8) makes it possible to improve the accuracy of modeling, even if they are used to identify only one of the polynomial kernels (9). Therefore, in this section, we restrict ourselves to the procedure for numerical identification of a nonstationary linear term from (9) based on test signals of the form (8).

As shown in Section 2, if we assume that identifying the kernel $K_2(s_1, s_2)$ in the quadratic term of the polynomial (9) has already been achieved in one way or another, then the substitution of (8) into (16) leads to (17). We present a difference scheme for finding a linear nonstationary kernel from (17) with a known right-hand side. To do this, we introduce on the interval $[0, T]$ a uniform grid $t_i = ih$, $i = \overline{0, N}$ and a subgrid $t_{i-1/2} = (i - 1/2)h$, $i = \overline{1, N}$, while we denote by $K^h_{i,j}$ the grid approximation of the kernel $K_1(t_i, t_j)$. To approximate the integrals in (17), we use the middle rectangle rule, taking into account $\nu \leq t$,

$$h \sum_{k=1}^{j} K^h_{i,\, k-1/2} \frac{t_{k-1/2}}{t_j} + h \sum_{k=j+1}^{i} K^h_{i,\, k-1/2} = q(t_i, t_j), i = \overline{1, N}, j = \overline{1, i}. \tag{28}$$

At each step $i = \overline{1, N}$, one has to solve a system of linear algebraic equations of dimension $(i \times i)$ with respect to $K^h_{i,\, k-1/2}$, $k = \overline{1, i}$.

Consider the application of the difference scheme (28) with help of a test example. Let the right side of (17) have the form

$$q(t, \nu) = t - \frac{\nu}{2} + \frac{5t^3}{24} - \frac{\nu^3}{48} + \frac{t\nu^2}{8} - \frac{t^2\nu}{4}. \tag{29}$$

This right side will correspond to the kernel $K_1(t, \nu)$ from example (21). Table 1 shows the results of numerical calculations obtained using the difference scheme (28). Here,

$$\varepsilon = \max_{1 \leq j \leq i \leq N} \left| K_1\left(t_i, t_{j-1/2}\right) - K^h_{i,\, j-1/2} \right|$$

denotes the errors of the numerical solution. The last column of the table shows the number of nodes in which the maximum error is achieved. The table shows that the proposed algorithm has a linear order of convergence.

Table 1. The error of the numerical solution to (17) with the right side (29).

h	*ε*	Node Number, (*i*, *j*)
1/8	0.00553385	(8, 2)
1/16	0.00268555	(16, 4)
1/32	0.00132243	(32, 8)
1/64	0.00065613	(64, 6)

Thus, the numerical construction of the quadratic Volterra polynomial using the quadrature of the middle rectangles can be implemented by the formula

$$h \sum_{j=1}^{i} K^h_1\left(t_i, t_{j-1/2}\right) x(t_j) + h^2 \sum_{k=1}^{i} \sum_{l=1}^{i} K^h_2(t_{k-1/2}, t_{l-1/2}) x(t_i - t_{k-1/2}) x(t_i - t_{l-1/2}) = g(t_i), i = \overline{1, N},$$

where the kernels $K_1^h\left(t_i, t_{j-1/2}\right)$ are obtained using the difference Equation (28).

5. Future Research

This section is devoted to interpreting the identification method for nonsymmetric kernel $K_1(t,s)$ presented in Section 2 for solving the reconstruction problem for symmetric function $K_2(s_1,s_2)$. For this, we introduce the system of integral Equation (9), where the functions $x(t)$ and $y(t)$ have the form

$$x(t) \equiv x_\nu^{\alpha_{1,2}}(t) = \begin{cases} 0, & t \le 0, \\ \alpha_{1,2}\frac{t}{\nu}, & 0 < t \le \nu, \\ \alpha_{1,2}, & t > \nu, \end{cases} \tag{30}$$

$$y(t) \equiv y_\nu^{\alpha_{1,2}}(t) = \begin{cases} 0, & t = 0, \nu = 0, \\ g^{\alpha_{1,2}}(t,\nu), & 0 < \nu \le t, \end{cases} \tag{31}$$

where $\alpha_1 \neq \alpha_2$, and $g_\nu^{\alpha_{1,2}}(t)$ is a sufficiently smooth function. Assuming that in (9) the kernel $K_2(s_1,s_2) = \varphi(s_1)\varphi(s_2)$ is a separable function, such that $\varphi(s) \in C_\Omega$, C_Ω is the space of continuous functions symmetric on the square $\Omega = \{s_1, s_2 : 0 \le s_1, s_2 \le T\}$; then, system (9) can be transformed to the form

$$\int\limits_0^t K_1(t,s)x(s)ds + \left(\int\limits_0^t \varphi(s)x(t-s)ds\right)^2 = y(t),$$

or, taking into account (30) and (31), into the system

$$\alpha_{1,2}\left(\int\limits_0^\nu K_1(t,s)\frac{s}{\nu}ds + \int\limits_\nu^t K_1(t,s)ds\right) + \alpha_{1,2}^2\left(\int\limits_0^\nu \varphi(t-s)\frac{s}{\nu}ds + \int\limits_\nu^t \varphi(t-s)ds\right)^2 = g^{\alpha_{1,2}}(t,\nu). \tag{32}$$

We introduce the following functions $f_1(t,\nu)$, $f_2(t,\nu)$:

$$f_1(t,\nu) = \int\limits_0^\nu K_1(t,s)\frac{s}{\nu}ds + \int\limits_\nu^t K_1(t,s)ds, \tag{33}$$

$$f_2(t,\nu) = \int\limits_0^\nu \varphi(t-s)\frac{s}{\nu}ds + \int\limits_\nu^t \varphi(t-s)ds. \tag{34}$$

The system of linear functional equations of the form (32), presented with the designations (33) and (34),

$$\begin{cases} \alpha_1 f_1(t,\nu) + \alpha_1^2 f_2^2(t,\nu) = g^{\alpha_1}(t,\nu), \\ \alpha_2 f_1(t,\nu) + \alpha_2^2 f_2^2(t,\nu) = g^{\alpha_2}(t,\nu), \end{cases}$$

where $\alpha_1 \neq \alpha_2$, has a unique solution

$$f_1(t,\nu) = \frac{\alpha_2^2 g^{\alpha_1}(t,\nu) - \alpha_1^2 g^{\alpha_2}(t,\nu)}{\alpha_1\alpha_2^2 - \alpha_1^2\alpha_2}, \tag{35}$$

$$f_2^2(t,\nu) = \frac{\alpha_1 g^{\alpha_2}(t,\nu) - \alpha_2 g^{\alpha_1}(t,\nu)}{\alpha_1\alpha_2^2 - \alpha_1^2\alpha_2}. \tag{36}$$

According to [35], the inversion formula for (33) has the form

$$K_1(t,\nu) = -2\frac{\partial f_1(t,\nu)}{\partial \nu} - \nu\frac{\partial^2 f_1(t,\nu)}{\partial^2 \nu},$$

or, introducing the differentiation operator $D_2 = 2\frac{\partial}{\partial v} + \nu\frac{\partial^2}{\partial^2 \nu_1}$,

$$K_1(t,\nu) = -D_2(f_1(t,\nu)).$$

Similarly, for (34) we have

$$\varphi(t-\nu) = -D_2(f_2(t,\nu)).$$

Here, the functions $f_1(t,\nu)$ and $f_2(t,\nu)$ are determined by (35) and (36), respectively.

6. Conclusions

This paper generalized the experience of using piecewise-specified test signals to identify nonlinear dynamic systems of the input–output type, represented as quadratic Volterra polynomials, taking into account the nonstationary properties of the object. The development of this direction is associated with the introduction of test signals with a rising edge, which are characteristic of input actions that occur in practice. The type of test signals introduced in this paper can be used to identify the Volterra kernels included in the quadratic Volterra polynomial.

The new approach to constructing a quadratic Volterra polynomial in the time domain is based on the use of physically realizable test signals, which is very promising for applications. Volterra integral equations of the first kind, to which the problem of identifying Volterra kernels is reduced, have explicit inversion formulas, which ensures the construction of high-speed computational procedures. These formulas include mixed partial derivatives. A new method is proposed for choosing the smoothing parameter of a cubic spline for a stable numerical calculation of the derivatives included in the constructed inversion formula. This choice of parameter provides effective filtering of measurement noise. The results of the computational experiment showed that the relative identification error is comparable to the relative error of the initial data error; at a noise level of the initial data of 2%, the methodological error in the identification of the Volterra kernel was 4.4%.

Author Contributions: Conceptualization, Y.V. and S.S.; methodology, Y.V. and S.S.; software, E.M., E.A. and V.B.; validation, Y.V., S.S., E.M., E.A. and V.B.; formal analysis, Y.V., S.S., E.M., E.A. and V.B.; investigation, Y.V. and S.S.; resources, Y.V., S.S., E.M., E.A. and V.B.; data curation, E.M. and V.B.; writing—original draft preparation, Y.V., S.S., E.M., E.A. and V.B.; writing—review and editing, Y.V., S.S., E.M., E.A. and V.B.; visualization, Y.V., S.S., E.M., E.A. and V.B.; supervision, Y.V., S.S., E.M., E.A. and V.B.; project administration, Y.V. and S.S.; funding acquisition, Y.V. and S.S. All authors have read and agreed to the published version of the manuscript.

Funding: This research was funded by Russian Science Foundation, grant number 22-21-00409.

Institutional Review Board Statement: Not applicable.

Informed Consent Statement: Not applicable.

Data Availability Statement: Not applicable.

Conflicts of Interest: The authors declare no conflict of interest.

References

1. Volterra, V. *A Theory of Functionals and of Integral and Integro-Differential Equations*; Dover Publications: New York, NY, USA, 1959; ISBN 0486442845.
2. Brunner, H. *Volterra Integral Equations: An Introduction to Theory and Applications*; Cambridge University Press: New York, NY, USA, 2017.
3. Apartsyn, A.S. *Nonclassical Linear Volterra Equations of the First Kind*; De Gruyter Publisher: Utrecht, The Netherlands; Boston, MA, USA, 2003. [CrossRef]
4. Boikov, I.V.; Krivulin, N.P. *Analytical and Numerical Methods for Identification of Dynamical Systems*; Penza State University: Penza, Russia, 2016.
5. Doyle, F., III; Pearson, R.; Ogunnaike, B. *Identification and Control Using Volterra Models*; Springer: Berlin, Germany, 2002.
6. Ogunfunmi, T. *Adaptive Nonlinear System Identification: The Volterra and Wiener Model Approaches*; Springer: Berlin, Germany, 2007.

7. Rugh, W.J. *Nonlinear System Theory: The Volterra/Weiner Approach*; John Hopkins Press: Baltimore, MD, USA, 1981.
8. Elloum, M.; Gassara, H.; Naifar, O. An Overview on Modelling of Complex Interconnected Nonlinear Systems. *Math. Probl. Eng.* **2022**, *2022*, 4789405. [CrossRef]
9. Szlobodnyik, G.; Szederkényi, G. Structural identifiability analysis of nonlinear time delayed systems with generalized frequency response functions. *Kybernetika* **2021**, *57*, 939–957. [CrossRef]
10. Wiener, N. *Nonlinear Problems in Random Theory*; The Technology Press of M.I.T.: New York, NY, USA; John Wiley & Sons, Inc.: Hoboken, NJ, USA, 1958.
11. Borys, A. On Modelling of Nonlinear Systems and Phenomena with the Use of Volterra and Wiener Series. *TransNav Int. J. Mar. Navig. Saf. Sea Transp.* **2015**, *9*, 91–98. [CrossRef]
12. Skyvulstad, H.; Petersen, Ø.W.; Argentini, T.; Zasso, A.; Øiseth, O. The use of a Laguerrian expansion basis as Volterra kernels for the efficient modeling of nonlinear self-excited forces on bridge decks. *J. Wind Eng. Ind. Aerodyn.* **2021**, *219*, 104805. [CrossRef]
13. Orcioni, S. Improving the approximation ability of Volterra series identified with a cross-correlation method. *Nonlinear Dyn.* **2014**, *78*, 2861–2869. [CrossRef]
14. Balassa, G. Estimating Scattering Potentials in Inverse Problems with a Non-Causal Volterra Model. *Mathematics* **2022**, *10*, 1257. [CrossRef]
15. Tsibizova, T.Y. Identification of nonlinear automatic control systems via Volterra filters. *Basic Res.* **2015**, *2*, 3070–3074.
16. Menshikov, B.N.; Priorov, A.L. Nonlinear echo-elimination on the basis of adaptive polynomial Volterra filter with a dynamically readjusted structure. *Digital Signal Processing* **2006**, *3*, 20–25.
17. Tsibizova, T.Y. Adaptive algorithm for identification of nonlinear systems by Volterra series. *Basic Res.* **2016**, *10*, 102–106.
18. Marmarelis, V.Z. Identification of nonlinear systems by use of nonstationary white-noise inputs. *Appl. Math. Model.* **1980**, *4*, 117–124. [CrossRef]
19. Mirri, D.; Iuculano, G.; Traverso, P.A.; Pasini, G.; Filicori, F. Non-linear dynamic system modelling based on modified Volterra series approaches. *Measurement* **2003**, *33*, 9–21. [CrossRef]
20. Liu, Q.; Xie, M.; Lim, M.-K. Volterra Series Models for Nonlinear System Control. In Proceedings of the 32nd ISR (International Symposium on Robotics), Seoul, Korea, 19–21 April 2001; pp. 1386–1391.
21. Medvedew, A.; Fomin, O.; Pavlenko, V.; Speranskyy, V. Diagnostic features space construction using Volterra kernels wavelet transforms. In Proceedings of the 2017 9th IEEE International Conference on Intelligent Data Acquisition and Advanced Computing Systems: Technology and Applications (IDAACS), Bucharest, Romania, 21–23 September 2017; pp. 1077–1081. [CrossRef]
22. Apartsyn, A.S. Nonclassical Volterra Equations of the First Kind in Integral Models of Dynamical Systems: Theory, Numerical Methods, Applications. Ph.D. Thesis, Irkutsk State University, Irkutsk, Russia, 2000.
23. Venikov, V.A.; Sukhanov, O.A.; Guseynov, A.F. Functional representation of subsystems in cybernetic modeling. In *Cybernetics of Electric Power Systems*; USSR Academy of Sciences: Bryansk, Russia, 1974; pp. 39–46.
24. Galin, N.M.; Zyabirov, F.I. Method for solving nonlinear problems of heat transfer using the Volterra functional series. In *Hydrodynamics and Heat Transfer in Single-Phase and Two-Phase Flows*; Moscow Energy Institute: Moscow, Russia, 1987; pp. 34–48.
25. Eykhoff, P. *System Identification: Parameter and State Estimation*; Wiley: Chichester, UK, 1974; p. 555.
26. Schetzen, M. Measurement of the Kernels of a Nonlinear System of Finite Order. *Int. J. Control* **1965**, *1*, 251–263. [CrossRef]
27. Danilov, L.V.; Matkhanov, P.N.; Filippov, E.S. *Theory of Nonlinear Electrical Circuits*; Energoatomizdat: Leningrad, Russia, 1990.
28. Venikov, V.A.; Sukhanov, O.A. *Cybernetic Models of Power Systems*; Energoizdat: Moscow, Russia, 1982.
29. Ljung, L. *System Identification: Theory for the User*; Prentice Hall, Inc.: Upper Sadle River, NJ, USA, 1987.
30. Pavlenko, S.V. Methods and Tools for Identifying Nonlinear Dynamic Systems Based on Volterra Models. Ph.D. Thesis, Odessa National Polytechnic University, Odessa, Ukraine, 2017.
31. Fujii, K.; Nakao, K. Identification of nonlinear dynamic systems without self–regulation using Volterra functional series. *Trans. Soc. Instrum. Control Eng.* **1971**, *7*, 129–136. [CrossRef]
32. Masri, M.M. Methods and Tools for Constructing Information Models of Nonlinear Dynamic Objects for Diagnostic Purposes. Ph.D. Thesis, Odessa National Polytechnic University, Odessa, Ukraine, 2015.
33. Pavlenko, V.D. Compensation method for identification of nonlinear dynamical systems in the form of Volterra kernels. *Proc. Odessa Polytech. Univ.* **2009**, *2*, 121–129.
34. Fedorova, A.N.; Fomin, A.A.; Pavlenko, V.D. The method of constructing multidimensional Volterra model of the oculo-motor apparatus. *Electr. Comput. Syst.* **2015**, *19*, 296–301. [CrossRef]
35. Solodusha, S.V. New Classes of Volterra Integral Equations of the First Kind Related to the Modeling of the Wind Turbine Dynamics. In Proceedings of the 2020 15th International Conference on Stability and Oscillations of Nonlinear Control Systems (Pyatnitskiy's Conference) (STAB), Moscow, Russia, 3–5 June 2020. [CrossRef]
36. Apartsyn, A.S. On increasing the accuracy of modeling the nonlinear dynamic systems with Volterra polynomials. *Electron. Modeling* **2001**, *23*, 3–12.
37. Voskoboynikov, Y.E.; Solodusha, S.V. Problem and algorithm for nonparametric identification of the combined quadratic Volterra polynomial using cubic splines. *Numer. Anal. Appl.* **2022**, *in press*.

38. Solodusha, S.V.; Orlova, I.V. Integral models of non-linear non-stationary systems and their applications. In Proceedings of the 2017 International Conference on Industrial Engineering, Applications and Manufacturing, ICIEAM 2017, Chelyabinsk, Russia, 16–19 May 2017; p. 8076419. [CrossRef]
39. Solodusha, S.V. Quadratic and cubic Volterra polynomials: Identification and application. *Vestn. St. Petersburg Univ. Appl. Math. Comput. Sci. Control. Processes* **2018**, *14*, 131–144. [CrossRef]
40. Tikhonov, A.N.; Arsenin, V.Y. *Solutions of Ill-Posed Problems*; Winston and Sons: Washington, DC, USA, 1977.
41. Voskoboynikov, Y.E.; Boeva, V.A. Non-parametric identification algorithms for complex engineering systems. *Sci. Bull. Novosib. State Tech. Univ.* **2020**, *4*, 47–64. [CrossRef]
42. Zavyalov, Y.S.; Kvasov, B.I.; Miroshnichenko, V.L. *Methods of Spline Functions*; Nauka: Moscow, Russia, 1980; p. 345.
43. Wang, Y. *Smoothing Splines Methods and Applications*; Ser. Monographs on Statistics and Applied Probability; CRC Press: Boca Raton, FL, USA, 2011; Volume 121, p. 347.
44. Voskoboynikov, Y.E.; Preobrazhensky, N.G.; Sedelnikov, A.I. *Mathematical Processing of Experiment in Molecular Gas Dynamics*; Nauka: Novosibirsk, Russia, 1984; p. 238.
45. Voskoboynikov, Y.E.; Boeva, V.A. Synthesis of smoothing cubic spline in non-parametric identification technical systems' algorithm. In Proceedings of the IOP Conference Series: Materials Science and Engineering. XIII International Scientific Conference Architecture and Construction, Novosibirsk, Russia, 22–24 September 2020; Institute of Physics Publishing: Bristol, UK, 2020; p. 012035. [CrossRef]
46. Voskoboynikov, Y.E.; Boeva, V.A. Stable algorithm for computing mixed derivatives in problems of nonparametric identification of nonlinear systems. *Mod. High Technol.* **2021**, *4*, 25–29. [CrossRef]
47. Rezghi, M.; Hosseini, S.M. A new variant of L-curve for Tikhonov regularization. *J. Comput. Appl. Math.* **2012**, *231*, 914–924. [CrossRef]
48. Cultrera, A.; Callegaro, L. A simple algorithm to find the L-curve corner in the regularization of ill-posed inverse problems. *IOP SciNotes* **2020**, *1*, 32–39. [CrossRef]
49. Voskoboynikov, Y.E.; Boeva, V.A. L-curve method for evaluating the optimal parameter of a smoothing cubic spline. *Int. Res. J.* **2021**, *11*, 6–13. [CrossRef]
50. Solodusha, S.V. Modeling heat exchangers by quadratic Volterra polynomials. *Autom. Remote Control* **2014**, *75*, 87–94. [CrossRef]
51. Apartsyn, A.S.; Solodusha, S.V.; Spiryaev, V.A. Modeling of Nonlinear Dynamic Systems with Volterra Polynomials: Elements of Theory and Applications. *Int. J. Energy Optim. Eng.* **2013**, *2*, 16–43. [CrossRef]